

## RARE SULFOSALTS FROM VULCANO, AEOLIAN ISLANDS, ITALY. IV. LILLIANITE

YURI S. BORODAEV

*Department of Geology, Moscow State University, Moscow 119899, Russia*

ANNA GARAVELLI

*Dipartimento Geomineralogico, University of Bari, Via E. Orabona 4, I-70125 Bari, Italy*

CARLO GARBARINO AND SILVANA M. GRILLO

*Dipartimento di Geoingegneria e Tecnologie Ambientali, University of Cagliari, Piazza d'Armi, I-09123 Cagliari, Italy*

NADEZHDA N. MOZGOVA

*IGEM, Russian Academy of Sciences, Staromonetny 35, Moscow 109017, Russia*

TATYANA YU. USPENSKAYA

*Shirshov Institute of Oceanology, Nakhimov Avenue, 36, Moscow 117851, Russia*

FILIPPO VURRO<sup>§</sup>

*Dipartimento Geomineralogico, University of Bari, Via E. Orabona 4, I-70125 Bari, Italy*

### ABSTRACT

Excellent samples of lillianite, a rare Pb–Bi sulfosalt, have been found around a high-temperature fumarole at the La Fossa crater, Vulcano Island, Italy. The mineral is associated with cannizzarite and, subordinately, with galenobismutite and rarer sulfosalts, as well as sphalerite and selenian galena. Lillianite occurs as laths and fibers up to 100–130  $\mu\text{m}$  in length, and about 20–30 and 1  $\mu\text{m}$  in width, respectively. Electron-microprobe analyses show that the lillianite from Vulcano has a composition close to the ideal  $\text{Pb}_3\text{Bi}_2\text{S}_6$ . Particularly interesting is the absence of Ag and Cu, which makes the lillianite from Vulcano unique in its purity, with only minor incorporation of Cd. Like in other sulfosalts from Vulcano, significant Se concentrations are invariably present (1.38–2.22 wt. %). Traces of chlorine were found in some crystals due to the high Cl activity in the fumaroles, and are noted for the first time. The general empirical formula,  $\text{Pb}_{3-x}\text{Bi}_{2+2x/3}(\text{S}_{6-y}\text{Se}_y)_{26}$ , reflects the narrow composition field for the lillianite from Vulcano. The X-ray powder-diffraction data, as well as microhardness and reflectance measurements, are given for distinct crystals with a different Pb/Bi value. The unit-cell constants are  $a$  13.576(9),  $b$  20.606(8),  $c$  4.119(2) Å for the crystal with Pb/Bi  $\approx$  1.50, and  $a$  13.56(1),  $b$  20.57(1),  $c$  4.115(2) Å for the one with Pb/Bi  $\approx$  1.41. In both films,  $h + l = 2n$  reflections correspond to the space group *Bbmm*. The lower value of microhardness of the Bi-rich sample may reflect the less well-ordered structure and the effect of the heterovalent substitution  $3\text{Pb}^{2+} \rightarrow 2\text{Bi}^{3+} + \square$ . A comparison between the lillianite from Vulcano and the synthetic homologous Phase III is also given.

*Keywords:* lillianite, Pb–Bi sulfosalts, fumaroles, Vulcano Island, Italy.

### SOMMAIRE

Nous avons trouvé d'excellents échantillons de lillianite, un sulfosel à Pb–Bi rare, autour d'une fumarole de haute température au cratère La Fossa, île de Vulcano, en Italie. Ce minéral est associé à la cannizzarite et, accessoirement, à la galénobismutite et des sulfosels plus rares, de même qu'à la sphalérite et la galène sélénifère. La lillianite se présente en plaquettes et en fibres atteignant 100–130  $\mu\text{m}$  en longueur, et environ 20–30 et 1  $\mu\text{m}$  en largeur, respectivement. Les données obtenues avec une microsonde électronique montrent que la lillianite de Vulcano a une composition proche du pôle  $\text{Pb}_3\text{Bi}_2\text{S}_6$ . L'absence de Ag et de

<sup>§</sup> E-mail address: f.vurro@geomin.uniba.it

Cu la rend unique, en fait, et seul le Cd est présent en quantités mineures. En revanche, des quantités importantes de Se sont invariablement présentes (1.38–2.22%, poids). Des traces de chlore ont été découvertes dans certains cristaux, et témoignent de l'activité élevée du Cl dans ce milieu. La formule générale empirique,  $\text{Pb}_{3-x}\text{Bi}_{2+2x/3}(\text{S}_{6-y}\text{Se}_y)_{\Sigma 6}$ , reflète l'intervalle limité de compositions. Nous incluons les données en diffraction X, méthode des poudres, de même que les mesures de microdureté et de réflectance, pour deux cristaux dont le rapport Pb/Bi diffère. Les paramètres réticulaires sont  $a$  13.576(9),  $b$  20.606(8),  $c$  4.119(2) Å pour un cristal ayant Pb/Bi  $\approx$  1.50, et  $a$  13.56(1),  $b$  20.57(1),  $c$  4.115(2) Å pour un autre ayant Pb/Bi  $\approx$  1.41. Dans les deux cas, les réflexions  $h + l = 2n$  correspondent au groupe spatial  $Bbmm$ . La valeur plus faible de la microdureté de l'échantillon plus riche en Bi pourrait résulter d'un désordre structural plus important, ou des effets de la substitution hétérovalente  $3\text{Pb}^{2+} \rightarrow 2\text{Bi}^{3+} + \square$ . Nous comparons aussi la lillianite de Vulcano à son homologue synthétique, la Phase III.

(Traduit par la Rédaction)

*Mots-clés:* lillianite, sulfosels à Pb–Bi, fumeroles, île de Vulcano, Italie.

## INTRODUCTION

Lillianite, ideally  $\text{Pb}_3\text{Bi}_2\text{S}_6$ , has a confused and complex history, as do almost all the other sulfosalts of the system  $\text{PbS–Bi}_2\text{S}_3$ . The mineral was first described as a variety of kobellite from the Lillian mine, Colorado (Keller & Keller 1885, Keller 1890). Later, the type material and material from other localities, initially described as lillianite, were found to be mixtures, although natural materials of composition very close to ideal  $\text{Pb}_3\text{Bi}_2\text{S}_6$  have been repeatedly described (Fleischer 1969, and references therein). Today, lillianite is considered as the natural analogue of synthetic Phase III (Otto & Strunz 1968).

The structure of lillianite was solved and redefined using both synthetic Phase III (Otto & Strunz 1968, Ohsumi *et al.* 1984), and natural crystals (Kupčik *et al.* 1969, Takagi & Takéuchi 1972). The structure consists of alternating slabs of galena-like structure parallel to  $(131)_{\text{PbS}}$ , which represents the reflection and contact plane of a chemical twin. Common sulfur atoms, which form bicapped trigonal prisms with the Pb atoms on the mirror plane (Makovicky 1977, 1981, Makovicky & Karup-Møller 1977a, b, Takéuchi 1997), connect the adjacent mirror-related layers. This structure acts as a parent type for the majority of the homologous series in sulfosalts belonging to the system  $\text{PbS–Bi}_2\text{S}_3\text{–Ag}_2\text{S}$ , as well as for some other sulfosalts (Makovicky & Karup-Møller 1977a).

Distinct homologues differ in the thickness of the layers, expressed by a number  $N$  of octahedra running diagonally across an individual layer and parallel to  $[011]_{\text{PbS}}$ . On this basis, each homologue is denoted as  $N_1N_2L$ , where  $N_1$  and  $N_2$  are the values of  $N$  for two mirror-related planes. Makovicky & Karup-Møller (1977a, b) showed that the chemical composition of the lillianite homologues can be expressed by means of the formula  $\text{Pb}_{N-1-2x}\text{Bi}_{2+x}\text{Ag}_x\text{S}_{N+2}$ , ( $Z = 4$ ), where  $N = (N_1 + N_2)/2$  and  $x$  is the coefficient in the substitution  $\text{Ag} + \text{Bi} \rightarrow 2\text{Pb}$ . Lillianite is denoted as  $4^4L$ , which means that its ideal structure has the values  $N_1 = N_2 = 4$ , and its general formula is  $\text{Pb}_{N-1}\text{Bi}_2\text{S}_{N+2}$ . The value of  $N$  may be calculated directly from the chemical data ( $N_{\text{chem}}$ ) or,

alternatively, it can be determined crystallographically ( $N_{\text{cryst}}$ ). The discrepancies between these values can be evaluated both in terms of the presence of metal vacancies in the layer of octahedra, as well as in terms of the presence of erroneously thin layers occurring randomly in the ordered sequence of layers (Makovicky & Karup-Møller 1977a, b).

In spite of the very abundant crystallographic investigations of the lillianite homologous series (LHS), natural lillianite has not been sufficiently studied, owing to its rarity and to its common intergrowth with various sulfosalts of Bi. Moreover, the mineral is usually considered as a stoichiometric compound with formula  $\text{Pb}_3\text{Bi}_2\text{S}_6$  (Mandarin 1999), but its synthetic analogue, Phase III of the system  $\text{PbS–Bi}_2\text{S}_3$ , has an extensive field of nonstoichiometry (Salanci & Moh 1969). Furthermore, the relationship between lillianite and synthetic Phase III is not entirely known and, in some cases, the formula  $\text{Pb}_8\text{Bi}_6\text{S}_{17}$  is reported as the formula of lillianite (Liu & Chang 1994). In addition, some of the physical properties attributed to lillianite, reflectance for example, were measured on materials that have not been confirmed by X-ray diffraction. Furthermore, in some cases, the data reported in handbooks are followed by reservations (Criddle & Stanley 1993). The set of X-ray data in PDF data files for lillianite is represented by that of Phase III of the system  $\text{PbS–Bi}_2\text{S}_3$  (Salanci & Moh 1969), and only a calculated set of data from a natural sample is given in the database (PDFWIN 71–0533).

Taking into account that almost all natural samples of lillianite contain small but significant quantities of Cu and Ag, an excellent subject of investigation is represented by the natural homogeneous Ag- and Cu-free lillianite from Vulcano, in the Aeolian Islands, Italy, first described by Mozgova with co-authors (1985) during a re-examination of the type sample of cannizzarite (collected at Vulcano in 1924). Later, new occurrences of lillianite were documented among the recent products of condensation in high-temperature fumaroles at the La Fossa crater of Vulcano (Garavelli 1994, Garavelli *et al.* 1997). The results of a mineralogical investigation on lillianite from Vulcano are presented in this paper.

## GEOLOGICAL SETTING AND OCCURRENCE

Vulcano Island and its fumarole system have been well described in previous papers (Borodaev *et al.* 1998, 2000, Vurro *et al.* 1999). Samples studied in this work were collected from fumarole FA, a high-temperature vent situated in the North inner slope of the La Fossa Crater (see previous papers of the series for more details). The temperature of this fumarole increased continuously since July 1988, when the present thermal "event" began ( $T = 430^{\circ}\text{C}$ ) to July 1993 ( $T = 665^{\circ}\text{C}$ ). After this thermal peak, a general decrease in temperature was recorded in the area ( $T = 490^{\circ}\text{C}$  in March 1995). Over the last five years, the temperature of this fumarole has not varied greatly, and in August 2000 the values ranged between 380 and  $400^{\circ}\text{C}$ .

Lillianite occurs in various samples of altered rocks covered by aggregates of crystals of sulfosalts. Samples described in this paper were collected in June 1994 on the ground around fumarole FA ( $T = 520^{\circ}\text{C}$ ), where the deposition of lillianite was particularly abundant.

Lillianite is closely associated with various sulfosalts in aggregates of tiny acicular and leafy crystals, silvery grey in color, with a metallic luster. The mineralogical association was quite similar in general terms, but not exactly the same, as in assemblages deposited around other high-temperature fumaroles at the crater since 1990 (Garavelli *et al.* 1997, Borodaev *et al.* 1998, 2000, Vurro *et al.* 1999). Our crystals of lillianite are associated with cannizzarite, a small quantity of galenobismutite and some rarer sulfosalts, as well as sphalerite (or wurtzite) and selenian galena. Bismuthinite seems absent.

## MORPHOLOGY

Under the scanning microscope (Cambridge Stereoscan 360), lillianite appears as laths as well as fibers measuring up to 100–300  $\mu\text{m}$  in length and about 20–30  $\mu\text{m}$  (laths), and about 1  $\mu\text{m}$  or less in width (fibers). Tiny tabular crystals of cannizzarite, partly enclosed in lillianite, are also rather abundant. Distinct crystals of sphalerite–wurtzite are also present on the surface of lillianite crystals (Fig. 1a). Some lillianite laths are well formed and terminated, with generally uniform and bright faces; these are weakly striated parallel to the elongation. Small crystals of ZnS occur sporadically on such crystals (Fig. 1b).

There are also corroded or skeletal prismatic crystals of lillianite with stepped surfaces without terminal faces, as well as skeletal remnants of partly dissolved lillianite as long prismatic crystals (Fig. 1c). The stepped surface reflects the perfect cleavage on  $\{100\}$ , which is characteristic of this mineral (Chukhrov 1960). A crust of newly formed Cl-bearing sulfides and sulfosalts, as well as halides (Fig. 1d) partly covers the skeletal remnants of lillianite, forming in places aggregates of idiomorphic crystals (Fig. 1c).

In SEM images, as well as in polished sections, some very interesting peculiarities of lillianite crystals are well displayed, like droplets on the tips of the tiny prismatic crystals. This evidence allows us to consider these crystals as whiskers (Wagner & Ellis 1965) growing through the vapor–liquid–solid (VLS) process.

## CHEMICAL DATA

Sixty-six electron-microprobe analyses of various crystals of lillianite, collected in June 1994 from fumarole FA were made on polished sections with two instruments: 45 analyses at the Centro Studi Geominerarie Mineralurgici, CNR, Cagliari using a ARL–SEM–95 instrument, and 21 analyses at Moscow State University with a Camebax SX–50 instrument. The analysis of some individual grains was repeated in the two laboratories. Analytical conditions were as follows: voltage 20 kV for both instruments, beam current 20 nA for the ARL–SEM–95 and 30 nA for the Camebax SX–50. Standards (emission lines) in both laboratories: PbS ( $\text{PbM}\alpha$ ,  $\text{SK}\alpha$ ), CdS ( $\text{CdL}\alpha$ ),  $\text{Bi}_2\text{S}_3$  ( $\text{BiM}\alpha$ ,  $\text{SK}\alpha$ ), metallic Ag ( $\text{AgL}\alpha$ ), CuS ( $\text{CuK}\alpha$ ); in Cagliari:  $\text{FeAsS}_2$  ( $\text{AsL}\alpha$ ), metallic selenium ( $\text{SeL}\alpha$ ), KCl ( $\text{ClK}\alpha$ ); in Moscow:  $\text{AgAsS}_2$ ,  $\text{Bi}_2\text{Se}_3$ ,  $\text{Pb}_5(\text{VO}_4)_3\text{Cl}$  with the same spectral lines as above. Detection limits are: Pb 0.10, Cd 0.14, Bi 0.10, As 0.08, S 0.02, Se 0.04, Cl 0.03, Ag 0.05, Cu 0.04 wt% at a confidence level of 99%. Analytical errors, at the same confidence level, are as follows: Pb 0.85, Cd 0.18, Bi 0.67, S 0.23, Se 0.10, and Cl 0.04 wt%.

The data obtained (Table 1) show that Pb, Bi and S concentrations range as follows (in wt%): Pb, 47.59–50.47 (average 49.11,  $\sigma$  0.5); Bi, 33.45–35.58 (average 34.59,  $\sigma$  0.4); S, 14.16–15.10 (average 14.70,  $\sigma$  0.2). In all cases, the lillianite is found to contain significant concentration of Se (1.38–2.22 wt%, average 1.71 wt%,  $\sigma$  0.2) like all the other sulfosalts from Vulcano (Mozgova *et al.* 1985, Garavelli 1994, Borodaev *et al.* 1998, 2000, Vurro *et al.* 1999). Small contents of rarer elements are sporadically present: Cd (up to 0.28 wt%) in 23 analyses and Cl (up to 0.06 wt%) in 18 analyses. Ag, Cu and As concentrations are below the detection limits in all cases. Traces of chlorine in lillianite crystals allow us to report for the first time the incorporation of Cl in Pb–Bi sulfosalts, very probably in substitution for S. Using the formula  $N_{\text{chem}} = -1 + \{\text{Bi}_i + (\text{Pb}_j - 1)/2\}^{-1}$  (Makovicky & Karup-Møller 1977a, Takéuchi 1997),  $N_{\text{chem}}$  was calculated for the 66 compositions of lillianite studied; the values range from 3.76 up to 4.00 (Table 1). It should be stressed that only one value equals 4.00, whereas the other values are non-integral and less than the theoretical value of one, according to the data reported by Makovicky & Karup-Møller (1977b) for the majority of natural samples of Ag-bearing lillianite. The ideal composition of lillianite,  $\text{Pb}_3\text{Bi}_2\text{S}_6$ , is also reported in Table 1.

Known compositions of lillianite from other localities generally contain quantities of Ag in substitution: up to 2.20 wt% in eastern Transbaikal, Russia (Ontoev 1959) and up to 2.68 wt% in China (Jiang *et al.* 1991, unpublished data quoted in Criddle & Stanley 1993). In this connection, we find it particularly interesting to note the absence of this element, as well as Cu, in the lillianite from Vulcano.

The results of all 66 analyses are plotted on the S(Se) – Bi – Pb(Cd) diagram (at.%) where they form a very small but significant field (Fig. 2). The field includes the ideal composition of lillianite,  $\text{Pb}_3\text{Bi}_2\text{S}_6$ , with a small shift to reflect the increasing Bi content. The compositional spread of lillianite from Vulcano corresponds to about 1.71 mol.%  $\text{Bi}_2(\text{S},\text{Se})_3$ . This spread clearly exceeds the analytical error ( $\approx 1.23$  mol.%  $\text{Bi}_2\text{S}_3$ ). This variation of composition is in good agreement with the common incidence of nonstoichiometry among Pb–Bi sulfosalts, due to the disordered distribution of  $\text{Pb}^{2+}$  and  $\text{Bi}^{3+}$  at the same structural sites (Mozgova 1985).

Formulae derived from thirteen selected sets of analytical data, representative of the whole compositional field of lillianite samples from Vulcano, are reported in Table 2. The list includes members with the highest and the lowest Pb/Bi atomic ratio (Table 2, No. 1–2 and 13, respectively) and the data obtained on the same grains both in Russia and in Italy (Table 2, No. 1–2, 4–5, 7–8). The very good agreement of the results obtained in two laboratories is remarkable. In the same table, the empirical chemical formulae, Pb/Bi atomic ratio, balance of valences, and the empirical chemical formulae with vacancies also are reported.

The empirical chemical formulae have been calculated on the basis of 11 atoms per formula unit (*apfu*). The balance of valences is rather good: deviations do not exceed 2.9% in all analyses. The atomic ratio Pb/Bi varies from 1.50 down to 1.38. Taking into account the deviations from integral values, the general empirical formula for lillianite studied can be expressed as follows:  $\text{Pb}_{3-x}\text{Bi}_{2+2x/3}(\text{S}_{6-y}\text{Se}_y)_{\Sigma 6}$  where  $0 \leq x \leq 0.1$  and  $y \approx$

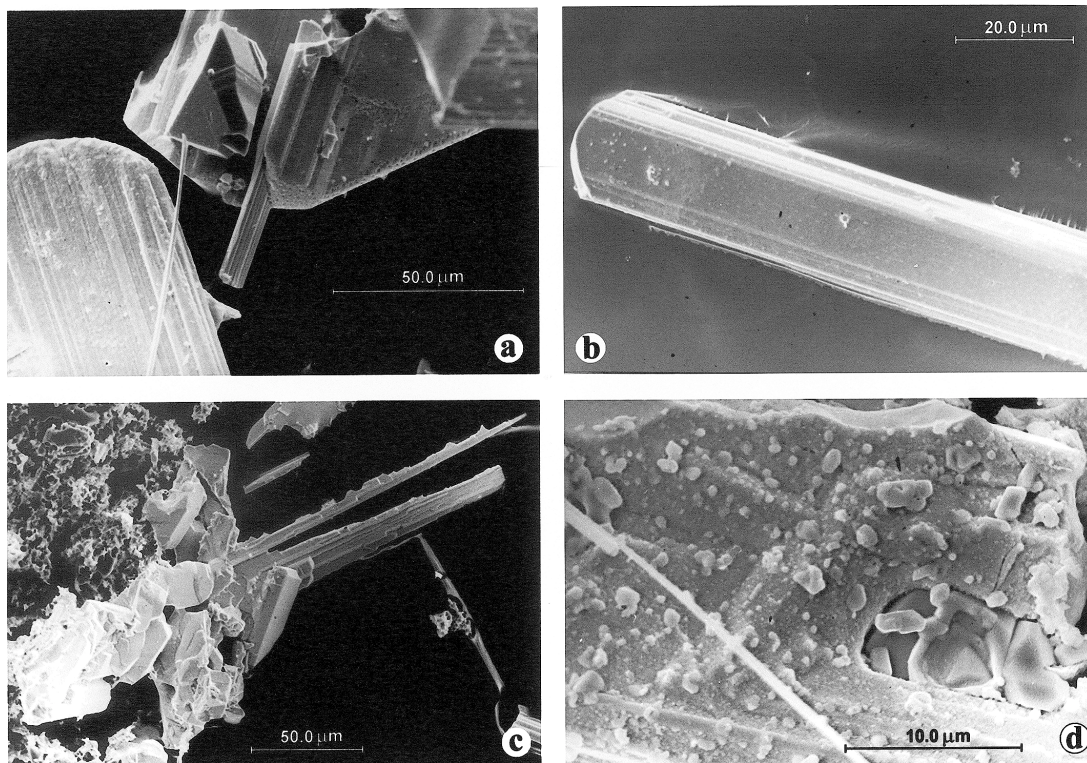


FIG. 1. Morphology and associations of lillianite crystals from Vulcano (Cambridge Stereoscan 360). a) Two morphological varieties of lillianite: elongate platy crystal and fibers; the tiny tabular crystal, partly included in the platy crystals of lillianite, is cannizzarite; the big crystal on the surface of lillianite is  $\text{ZnS}$ . b) Well-formed lath of lillianite with terminal faces; faces are weakly striated parallel to the elongation. Some small tetrahedra of  $\text{ZnS}$  are visible on the surface of the lillianite crystals. c) Corroded long prismatic crystals of lillianite; aggregates of idiomorphic crystals of Cl- and S-bearing minerals can be seen at the base of the skeletal remnants of partly dissolved lillianite. d) A detail of the crust consisting of newly formed Cl- and S-bearing minerals covering a corroded crystal of lillianite.

0.25. There is no clear correlation between  $x$  and  $y$  coefficients.

The empirical chemical formulae with vacancies ( $\square$ ) expressed have been calculated from the empirical chemical formulae considering the substitution  $3\text{Pb} \rightarrow 2\text{Bi} + \square$  as being mainly responsible for nonstoichiometry in lillianite from Vulcano. The proportion of vacancies does not exceed 0.04 per formula unit.

#### OPTICAL PROPERTIES AND MICROHARDNESS

Under reflected light in polished sections, lillianite is white. The bireflectance is weak, but varies noticeably, even in a single crystal. Reflection pleochroism is absent. The anisotropy is distinct, but without color effect. Quantitative data on reflectance were obtained for lillianite on the largest crystals that had been well polished and pre-analyzed in both laboratories [Table 2, No. 4–5; Pb/Bi (atomic) = 1.44]. Reflectance was measured

in air from 420 to 700 nm using an automatic MSFU–312L polarization microspectrophotometer (LOMO, Saint Petersburg), with Si as standard and a  $20 \times 0.40$  objective (Table 3). The results for the spectral curves obtained for this crystal, as well as the standard curve [Jiang *et al.* (1991), unpublished data quoted in Criddle & Stanley (1993)] are plotted in Figure 3. The standard reflectivity curve  $R_3$  occupies an intermediate position between  $R_1$  and  $R_2$ . Taking into account the analytical error (1.5%), the reflectance of the lillianite from Vulcano is rather close to the standard data. Bireflectance is about 4% at 560 nm.

The microhardness was measured on two crystals of somewhat different bulk composition, one with Pb/Bi  $\approx 1.50$  (Table 2, No. 1–2), and the other with Pb/Bi  $\approx 1.41$  (Table 2, No. 7–8). An indentation-hardness tester (PMT–3M) was used with various light loads (up to 100 g), as previously recommended by Shcherbachev

TABLE 1. LILLIANITE FROM VULCANO: CHEMICAL DATA AND  $N_{\text{chem}}$  VALUES

No.	No. anal. Table 2	Pb	Cd	Bi	S	Se	Cl	Tot	$N_{\text{chem}}$
1		48.84	0.24	34.63	14.77	1.56	0.00	100.04	3.87
2		48.91	0.20	34.67	14.70	1.97	0.00	100.45	3.87
3		49.42	0.00	34.47	14.58	1.98	0.00	100.45	3.89
4		48.98	0.28	34.50	14.72	1.57	0.00	100.05	3.89
5		48.90	0.00	34.96	14.62	1.97	0.00	100.45	3.82
6		48.73	0.00	34.59	14.64	1.76	0.00	99.72	3.84
7		48.98	0.00	34.74	14.98	2.07	0.00	100.77	3.84
8		48.98	0.25	34.67	14.98	1.56	0.00	100.44	3.88
9		48.55	0.00	33.68	14.85	2.12	0.00	99.20	3.91
10		48.68	0.00	34.70	14.65	1.99	0.00	100.02	3.83
11		48.93	0.00	34.79	14.77	1.65	0.00	100.14	3.84
12		49.52	0.00	34.92	14.51	1.89	0.00	100.84	3.86
13		49.61	0.00	34.33	14.46	2.22	0.00	100.62	3.91
14		49.31	0.00	34.17	14.34	1.88	0.00	99.70	3.91
15		49.74	0.00	34.14	14.35	2.08	0.00	100.31	3.94
16		49.22	0.00	34.37	14.50	2.08	0.00	100.17	3.89
17		48.92	0.16	35.11	14.66	1.75	0.00	100.60	3.83
18		48.86	0.00	34.97	14.53	1.87	0.00	100.23	3.82
19		49.01	0.00	34.92	14.58	2.07	0.00	100.58	3.83
20	3	49.25	0.00	33.53	14.80	1.43	0.00	99.01	3.96
21		49.29	0.00	34.83	14.76	1.52	0.00	100.40	3.85
22		49.29	0.17	34.52	14.82	1.60	0.00	100.40	3.90
23		49.15	0.17	34.42	15.04	1.48	0.00	100.26	3.90
24		48.93	0.00	34.26	15.04	1.54	0.00	99.77	3.88
25	4	49.63	0.00	34.90	15.10	1.63	0.00	101.26	3.87
26		48.89	0.00	34.76	14.41	1.95	0.00	100.01	3.84
27		49.09	0.00	34.52	14.34	1.83	0.00	99.78	3.87
28		48.32	0.00	34.70	14.16	1.81	0.00	98.99	3.81
29		48.56	0.00	34.46	14.58	1.57	0.00	98.97	3.84
30	10	47.59	0.00	34.42	14.40	1.80	0.00	98.21	3.79
31		49.75	0.00	34.86	14.89	1.45	0.00	100.95	3.88
32		49.03	0.00	34.81	14.65	1.70	0.00	100.19	3.84
33		49.09	0.00	34.60	14.79	1.72	0.00	100.20	3.86
34		48.82	0.00	34.87	14.37	1.78	0.00	99.84	3.82
35		48.84	0.00	34.77	14.69	1.73	0.00	100.03	3.83
36		48.68	0.00	34.63	14.42	1.72	0.00	99.45	3.84
37	1	50.10	0.21	34.07	14.76	1.85	0.00	100.99	3.99
38		49.28	0.00	34.75	14.75	1.60	0.00	100.38	3.86
39	11	48.51	0.00	34.98	14.75	1.83	0.00	100.07	3.80
40		48.62	0.00	34.60	14.81	1.49	0.00	99.52	3.83
41	7	48.80	0.00	35.00	14.56	1.52	0.00	99.88	3.81
42	9	48.55	0.00	35.29	14.67	1.70	0.00	100.21	3.77
43		49.92	0.00	34.62	14.85	1.83	0.00	101.22	3.91
44		48.94	0.27	34.49	14.80	1.83	0.00	100.33	3.89
45	6	48.58	0.19	34.56	14.48	1.99	0.06	99.86	3.86

The analyses were made at the University of Cagliari with an ARL–SEMQ–95 electron microprobe. Results of the analyses are expressed in wt %.

TABLE 1 (continued). LILLIANITE FROM VULCANO: CHEMICAL DATA AND  $N_{\text{chem}}$  VALUES

No.	No. anal. Table 2	Pb	Cd	Bi	S	Se	Cl	Tot	$N_{\text{chem}}$
46		50.47	0.05	34.60	14.61	1.51	0.04	101.28	3.95
47		48.60	0.11	34.33	14.68	1.38	0.02	99.12	3.87
48		49.02	0.13	34.03	14.79	1.62	0.00	99.59	3.92
49		49.04	0.03	34.57	14.59	1.74	0.00	99.98	3.86
50	12	48.57	n.d.	35.24	14.61	1.56	0.05	100.03	3.78
51		50.13	0.01	34.53	14.96	1.63	0.04	101.30	3.93
52		49.13	0.00	35.58	14.91	1.76	0.02	101.40	3.79
53	13	48.10	n.d.	35.21	14.79	1.54	0.04	99.68	3.76
54		49.52	0.03	35.33	14.95	1.54	0.01	101.39	3.83
55	8	48.45	0.20	34.60	14.76	1.58	0.05	99.64	3.85
56		49.66	0.04	34.48	14.77	1.75	0.03	100.77	3.91
57		49.22	0.16	34.64	14.90	1.53	0.05	100.55	3.88
58		49.62	0.13	33.90	15.01	1.47	0.05	100.18	3.97
59		49.35	0.07	34.30	14.32	1.68	0.04	99.76	3.91
60		49.55	0.00	34.76	14.62	1.58	0.04	100.56	3.88
61		50.31	0.00	33.80	14.67	1.48	0.04	100.30	4.00
62		50.12	0.21	34.56	14.78	1.61	0.03	101.31	3.95
63		49.09	0.05	34.80	14.86	1.54	0.03	100.37	3.85
64	5	49.06	n.d.	34.41	14.84	1.54	0.00	99.85	3.88
65	2	49.33	n.d.	33.45	14.92	1.58	0.05	99.33	3.97
66		49.11	0.00	34.19	14.94	1.54	0.00	99.78	3.90

The analyses were made in Russia with a Camebax SX–50 electron microprobe. Results of the analyses are expressed in wt%; n.d.: not determined.

#### Minimum, Maximum, and Standard Deviation

		Pb	Cd	Bi	S	Se	Cl	$N_{\text{chem}}$
		<i>Min</i>	47.59	0.00	33.53	14.16	1.43	0.00
	<i>Max</i>	50.10	0.28	35.29	15.10	2.22	0.06	3.99
	<i>Average</i>	49.01	0.05	34.61	14.66	1.78	0.00	3.86
	<i>St Dev</i>	0.45	0.09	0.34	0.22	0.21	0.01	0.04
Italy: 45 analyses	<i>Min</i>	47.59	0.00	33.45	14.16	1.38	0.00	3.76
	<i>Max</i>	50.47	0.21	35.58	15.01	1.76	0.05	4.00
	<i>Average</i>	49.31	0.07	34.54	14.78	1.58	0.03	3.89
	<i>St Dev</i>	0.62	0.07	0.52	0.17	0.09	0.02	0.07
Russia: 21 analyses	<i>Min</i>	48.10	0.00	33.45	14.32	1.38	0.00	3.76
	<i>Max</i>	50.47	0.21	35.58	15.01	1.76	0.05	4.00
	<i>Average</i>	49.31	0.07	34.54	14.78	1.58	0.03	3.89
	<i>St Dev</i>	0.62	0.07	0.52	0.17	0.09	0.02	0.07
Whole set of data: 66 analyses	<i>Min</i>	47.59	0.00	33.45	14.16	1.38	0.00	3.76
	<i>Max</i>	50.47	0.28	35.58	15.10	2.22	0.06	4.00
	<i>Average</i>	49.11	0.05	34.59	14.70	1.71	0.01	3.87
	<i>St Dev</i>	0.52	0.09	0.40	0.21	0.20	0.02	0.05

#### Ideal composition

	Pb	Cd	Bi	S	Se	Cl	Tot	$N_{\text{chem}}$
$\text{Pb}_2\text{Bi}_2\text{S}_6$	50.46	-	33.93	15.61	-	-	100.00	4.00

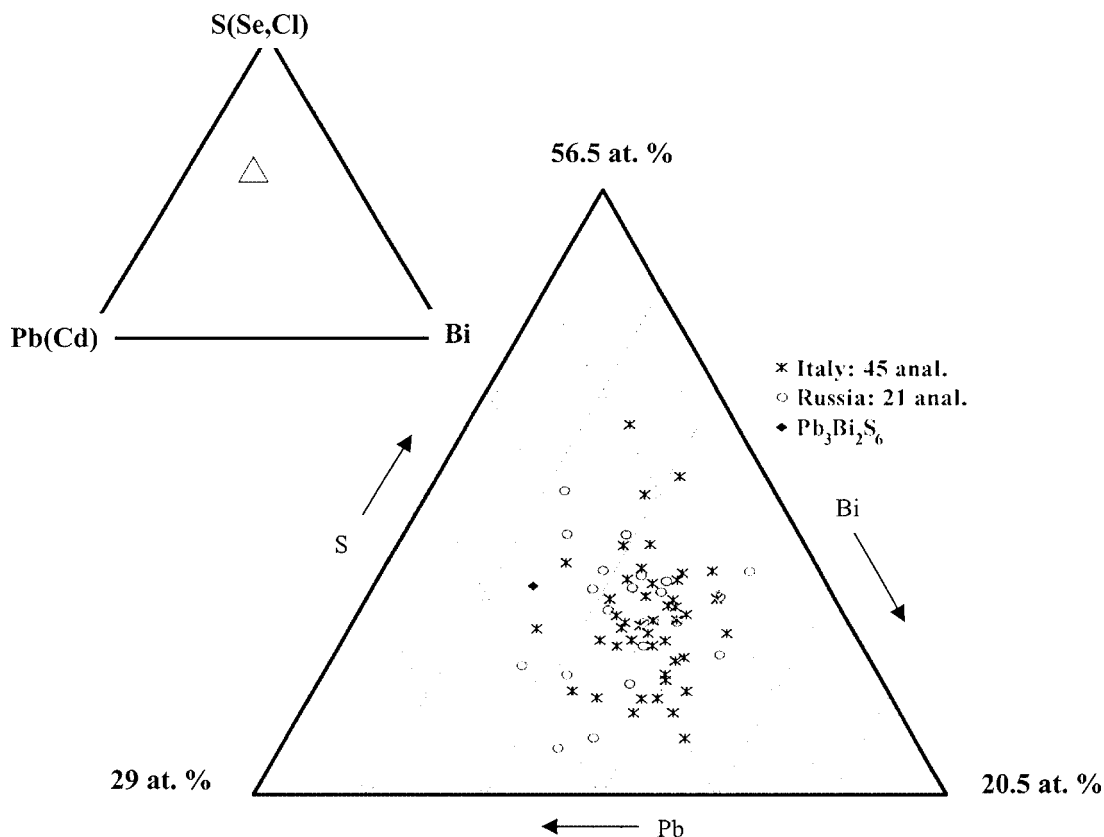


FIG. 2. Projection of the composition field of lillianite (atom %) and the ideal  $\text{Pb}_3\text{Bi}_2\text{S}_6$  composition in the diagram  $\text{S}(\text{Se,Cl}) - \text{Bi} - \text{Pb}(\text{Cd})$ . Increment = 0.5 at. %.

(1998). The data chosen for comparison were obtained with small loads (15 and 20 g, respectively), because their indentations did not induce cracks, which could influence the results. The values of microhardness (in  $\text{kg}/\text{mm}^2$ ) seem to decrease with an increase in the Bi content: from 234 and 210 (load 15 and 20 g, respectively) for the crystal with  $\text{Pb}/\text{Bi} \approx 1.50$  to 151 and 156 (load 15 and 20 g, respectively) for the crystal with  $\text{Pb}/\text{Bi} \approx 1.41$ .

#### DIFFRACTION DATA

Electron-diffraction data for lillianite were obtained with a JEM-100C microscope. The results are displayed in Figure 4. Lillianite appears as irregular fragments of elongate platy particles. Two different selected-area electron-diffraction patterns (SAED) were obtained. The first type of SAED pattern (Fig. 4a) allowed us to determine  $b \approx 20.2$  and  $c \approx 4.0$  Å. The preferred orientation of particles, parallel to  $b$  and  $c$ , is due to perfect cleav-

age  $\{100\}$ , and has not allowed us to determine the parameter  $a$ . The presence of reflections along  $b^*$  according to  $k = 2n$  agrees with space group  $Bbmm$  found for Phase III, synthetic lillianite (Otto & Strunz 1968), as well as for analogous natural material (Kupčik *et al.* 1969). The second type of SAED pattern is analogous to the first, with some diffuse streaks parallel to  $b^*$  (Fig. 4b), indicative of disorder in the structure.

Two chemically analyzed crystals of lillianite, extracted from a polished section under the microscope (Table 2, No. 1–2 and 7–8), were used to obtain X-ray powder-diffraction data. A Debye–Scherrer camera 114 mm in diameter (unfiltered Fe-radiation, Si as a standard) was used; the relative intensities of lines were estimated visually. The  $d$  values of the reflections were corrected with reference to a silicon internal standard. The results are given in Table 4 in comparison with a selection of lines from the calculated powder diagram (PDFWIN No. 71–0533) from the crystal structure obtained on natural lillianite by Takagi & Takéuchi (1972),

TABLE 2. EMPIRICAL CHEMICAL FORMULAE FOR LILLIANITE FROM VULCANO, SAMPLED AT FUMAROLE FA: RESULTS OF SELECTED REPRESENTATIVE ANALYSES

No.	No. anal. Table 1	Empirical chemical Formulae calculated on the basis of 11 at.	Pb/Bi	Balance of valences	Empirical chemical formulae with vacancies $Pb_{2-3x}Bi_{2+2x}□_xS_6$
1	37	$(Pb_{2.99}Cd_{0.02})_{\Sigma 3.01}Bi_{2.01}(S_{5.69}Se_{0.29})_{\Sigma 5.98}$	1.50	0.75	$(Pb_{2.97}Cd_{0.02})_{\Sigma 2.99}Bi_{2.00}□_{0.00}(S_{5.71}Se_{0.29})_{\Sigma 6.00}$
2	65	$Pb_{2.96}Bi_{1.99}(S_{5.79}Se_{0.25}Cl_{0.02})_{\Sigma 6.06}$	1.49	-1.57	$Pb_{2.96}Bi_{2.01}□_{0.00}(S_{5.73}Se_{0.25}Cl_{0.02})_{\Sigma 6.00}$
3	20	$Pb_{2.98}Bi_{2.01}(S_{5.78}Se_{0.23})_{\Sigma 6.01}$	1.48	-0.25	$Pb_{2.98}Bi_{2.01}□_{0.01}(S_{5.77}Se_{0.23})_{\Sigma 6.00}$
4	25	$Pb_{2.93}Bi_{2.04}(S_{5.77}Se_{0.25})_{\Sigma 6.02}$	1.44	-0.50	$Pb_{2.93}Bi_{2.05}□_{0.02}(S_{5.75}Se_{0.25})_{\Sigma 6.00}$
5	64	$Pb_{2.95}Bi_{2.05}(S_{5.76}Se_{0.24})_{\Sigma 6.00}$	1.44	0.42	$Pb_{2.94}Bi_{2.04}□_{0.02}(S_{5.76}Se_{0.24})_{\Sigma 6.00}$
6	45	$(Pb_{2.93}Cd_{0.02})_{\Sigma 2.95}Bi_{2.07}(S_{5.65}Se_{0.32}Cl_{0.02})_{\Sigma 5.99}$	1.43	1.25	$(Pb_{2.91}Cd_{0.02})_{\Sigma 2.93}Bi_{2.05}□_{0.02}(S_{5.66}Se_{0.32}Cl_{0.02})_{\Sigma 6.00}$
7	41	$Pb_{2.96}Bi_{2.10}(S_{5.76}Se_{0.24})_{\Sigma 5.94}$	1.41	2.86	$Pb_{2.90}Bi_{2.07}□_{0.03}(S_{5.76}Se_{0.24})_{\Sigma 6.00}$
8	55	$(Pb_{2.91}Cd_{0.02})_{\Sigma 2.93}Bi_{2.06}(S_{5.74}Se_{0.25}Cl_{0.02})_{\Sigma 6.01}$	1.42	0.33	$(Pb_{2.90}Cd_{0.02})_{\Sigma 2.92}Bi_{2.05}□_{0.03}(S_{5.74}Se_{0.25}Cl_{0.02})_{\Sigma 6.00}$
9	42	$Pb_{2.92}Bi_{2.11}(S_{5.71}Se_{0.27})_{\Sigma 5.98}$	1.38	1.76	$Pb_{2.88}Bi_{2.08}□_{0.04}(S_{5.71}Se_{0.27})_{\Sigma 6.00}$
10	30	$Pb_{2.92}Bi_{2.09}(S_{5.70}Se_{0.29})_{\Sigma 5.99}$	1.40	1.09	$Pb_{2.89}Bi_{2.08}□_{0.04}(S_{5.71}Se_{0.29})_{\Sigma 6.00}$
11	39	$Pb_{2.91}Bi_{2.08}(S_{5.72}Se_{0.29})_{\Sigma 6.01}$	1.40	0.33	$Pb_{2.90}Bi_{2.07}□_{0.04}(S_{5.71}Se_{0.29})_{\Sigma 6.00}$
12	50	$Pb_{2.93}Bi_{2.11}(S_{5.70}Se_{0.25}Cl_{0.02})_{\Sigma 5.97}$	1.39	2.09	$Pb_{2.89}Bi_{2.08}□_{0.04}(S_{5.73}Se_{0.25}Cl_{0.02})_{\Sigma 6.00}$
13	53	$Pb_{2.89}Bi_{2.10}(S_{5.75}Se_{0.24}Cl_{0.02})_{\Sigma 6.01}$	1.38	0.75	$Pb_{2.87}Bi_{2.09}□_{0.04}(S_{5.74}Se_{0.24}Cl_{0.02})_{\Sigma 6.00}$

No. 1,3,4,6,7,9-11 : ARL-SEM95 electron microprobe; No. 2,5,8,12,13 : CAMEBAX SX-50 electron microprobe.

No. 1-2 , 4-5, 7-8 were performed on the same grains. Valence in % was calculated with formula :  $[\sum(val^+) - \sum(val^-)] \times 100 / \sum(val^+)$

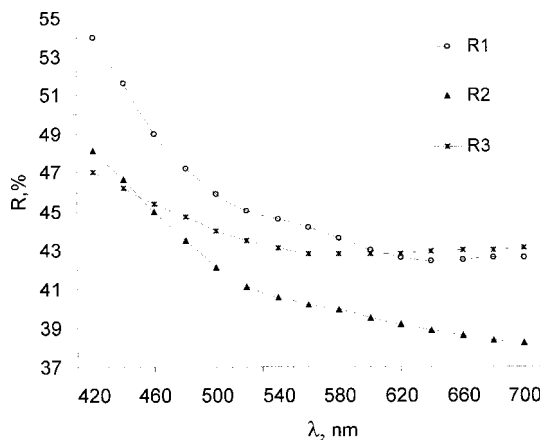


FIG. 3. Reflectance spectra in air for lillianite from the fumarole FA and standard data R3 [Jiang *et al.* (1991), unpublished data quoted in Criedle & Stanley (1993).

as well as those of synthetic Phase III (Otto & Strunz 1968) and those of natural lillianite from the Bukuka tungsten deposit, eastern Transbaikal, Russia (Klyakhin & Dmitrieva 1968). The cell constants were refined by the least-squares method on the basis of 24 reliable reflections indexed according to the calculated powder diagram (PDFWIN No. 71-0533). Four reflections were used in the calculation, with double indexes. The cell constants thus determined are (Å):  $a$  13.576(9),  $b$  20.606(8),  $c$  4.119(2) for the crystal with Pb/Bi  $\approx$  1.50, and  $a$  13.56(1),  $b$  20.57(1),  $c$  4.115(2) for the one with Pb/Bi  $\approx$  1.41. In both films,  $h + l = 2n$  reflections correspond to the space group  $Bbmm$ .

TABLE 3. REFLECTANCE DATA FOR LILLIANITE (Pb/Bi  $\approx$  1.44) FROM VULCANO

$\lambda$ , nm	$R'_1$	$R'_2$	$\lambda$ , nm	$R'_1$	$R'_2$
420	54.00	48.12	560	44.15	40.20
440	51.62	46.66	580	43.61	39.90
460	49.05	44.96	600	43.01	39.52
480	47.23	43.47	620	42.58	39.16
500	45.89	42.10	640	42.42	38.88
520	45.06	41.10	660	42.50	38.65
540	44.58	40.54	680	42.59	38.39
			700	42.62	38.23

\* Standard: Si. Reflectance data are expressed in %.

The results obtained for the two crystals from Vulcano (Table 4) are very close, as well as to the published data for synthetic Phase III reported in the PDF file 29-763 on synthetic lillianite (Otto & Strunz 1968) and to natural lillianite from Bukuka (Klyakhin & Dmitrieva 1968). Small differences between our data and the published values may be caused by small variations in composition. For the lillianite from Vulcano, values of  $d$  and cell parameter  $b$  of the Bi-rich member are somewhat smaller than those of the Pb-rich one, whereas the differences between the other cell parameters ( $a$  and  $c$ ) lie within error. We note also that the strong broad line with  $d = 3.41$  Å ( $I = 8$ ) in the Bi-rich crystal is split into two reflections with  $d = 3.45$  and  $3.41$  Å ( $I = 8$ ) in the Pb-rich crystal (Table 4). It is evidently a consequence of a greater degree of order in the crystal structure of lillianite with composition close to the ideal one.

TABLE 4. X-RAY POWDER-DIFFRACTION DATA FOR LILLIANITE AND SYNTHETIC PHASE III

I			II			III			IV			V		
<i>I</i> / <i>I</i> <sub>0</sub>	<i>d</i> <sub>meas</sub>	<i>d</i> <sub>cal</sub>	<i>I</i> / <i>I</i> <sub>0</sub>	<i>d</i> <sub>meas</sub>	<i>d</i> <sub>cal</sub>	<i>hkl</i>	<i>d</i> <sub>cal</sub>	<i>I</i>	<i>I</i> / <i>I</i> <sub>0</sub>	<i>d</i> <sub>meas</sub>	<i>I</i> / <i>I</i> <sub>0</sub>	<i>d</i> <sub>meas</sub>		
5	4.06	4.104	5	4.07	4.097	2 4 0	4.0794	177	35	4.1	3	4.05		
5	3.90	3.942	5	3.89	3.938	1 0 1	3.9274	41	20	3.934	-	-		
3	3.77	3.871	3	3.76	3.867	1 1 1	3.8569	32	10	3.880	3	3.85		
6	3.68	3.681	6	3.67	3.677	1 2 1	3.6663	289	40	3.678	2	3.66		
10	3.52	3.523	10	3.52	3.517	2 5 0	3.5005	999	100	3.523	9	3.50		
8b	3.45	3.434	-	-	3.428	0 6 0	-	-	-	-	-	-		
8b	3.41	3.419	8b	3.41	3.415	1 3 1	3.4030	570	70	3.419	6	3.39		
-	-	3.394	-	-	3.390	4 0 0	3.3887	272	30	3.384	-	-		
3	3.35	3.349	5	3.32	3.345	4 1 0	3.3383	168	30	3.326	-	-		
5	3.21	3.224	5	3.21	3.220	4 2 0	3.2124	40	10	3.211	3	3.21		
2	3.13	3.130	3	3.13	3.126	1 4 1	3.1145	120	30	3.128	-	-		
5	3.07	3.064	5	3.06	3.059	2 6 0	3.0441	150	30	3.060	2	3.04		
8	3.010	3.013	8	3.004	3.010	3 1 1	3.0029	443	60	3.005	6	3.00		
9	2.923	2.921	9	2.915	2.918	3 2 1	2.9103	583	80	2.913	9	2.91		
7	2.784	2.785	7	2.784	2.781	3 3 1	2.7733	317	60	2.778	6	2.77		
4	2.705	2.701	4	2.699	2.696	2 7 0	2.6888	103	40	2.699	4	2.68		
1	2.592	2.589	1	2.590	2.586	1 6 1	2.5742	5	-	-	-	-		
-	-	2.576	-	-	2.571	0 8 0	2.5563	24	5	2.575	1	2.57		
1	2.447	2.450	1	2.447	2.446	3 5 1	2.4377	21	10	2.447	-	-		
6b	2.361	2.359	6b	2.356	2.355	1 7 1	2.3444	131	40	2.357	6	2.34		
4b	2.279	2.279	4b	2.271	2.276	3 6 1	2.2670	5	-	-	3	2.26		
-	-	2.224	-	-	2.220	4 7 0	2.2113	16	5	2.220	-	-		
1	2.185	2.214	1	2.185	2.211	5 2 1	2.2064	10	-	-	-	-		
7b	2.153 {	2.156 {	7b	2.149 {	2.153 {	1 8 1	2.1424	372	50	2.156	-	-		
-	2.149	2.146	-	2.146	2.146	6 3 0	-	-	30	2.147	10	2.14		
6	2.116	2.117	3	2.113	2.114	3 7 1	2.1051	3	-	-	-	-		
-	-	2.072	-	-	2.069	6 4 0	2.0668	284	30	2.065	-	-		
-	-	2.075	-	-	2.072	5 4 1	2.0638	253	60	2.070	-	-		
8b	2.062 {	2.061 {	7b	2.057 {	2.058 {	0 10 0	2.0451	165	-	-	-	-		
-	2.060	2.058	-	2.057	2.058	0 0 2	2.0520	217	50	2.058	10	2.05		
4	1.984 {	1.986 {	4	1.982 {	1.984 {	5 5 1	1.9779	116	50	1.9815	-	-		
-	1.983	1.983	-	1.981	1.981	6 5 0	-	-	-	-	-	-		
-	-	1.980	-	-	1.977	1 9 1	1.9668	37	50	1.9786	-	-		
3	1.969	1.967	3	1.961	1.964	3 8 1	-	-	30	1.9645	6b	1.955		
-	-	1.962	-	-	1.960	2 1 2	1.9554	112	-	-	-	-		
1b	1.897 {	1.898 {	1b	1.893 {	1.895 {	4 9 0	1.8864	55	20	1.8978	-	-		
-	1.894	1.894	-	1.892	1.892	2 3 2	-	-	-	-	-	-		
-	-	1.892	-	-	1.889	5 6 1	1.8834	61	20	1.8867	4	1.875		
-	-	1.889	-	-	1.887	6 6 0	-	-	-	-	-	-		
-	-	1.841	-	-	1.839	2 4 2	1.8334	28	5	1.8374	-	-		
2b	1.832	1.830	3b	1.830	1.827	3 9 1	1.8191	71	20	1.8281	1	1.820		
-	-	1.826	-	-	1.823	1 10 1	1.8139	40	-	-	-	-		
5b	1.804	1.806	2b	1.802	1.803	2 11 0	1.7927	23	-	-	-	-		
-	-	1.796	-	-	1.794	5 7 1	1.7874	58	20	1.7911	3	1.785		
-	-	1.794	-	-	1.791	6 7 0	-	-	-	-	-	-		
4	1.779	1.778	6	1.776	1.776	2 5 2	1.7702	215	70	1.7765	6	1.778		
-	-	1.761	-	-	1.759	4 0 2	1.7545	65	-	-	-	-		
-	-	1.761	-	-	1.759	4 10 0	-	-	30	1.7590	6	1.747		
3b	1.754	1.754	4b	1.753	1.752	4 1 2	1.7502	144	20	1.7499	-	-		
<i>a</i> (Å) = 13.576(9)			<i>a</i> (Å) = 13.56(1)			<i>a</i> (Å) = 13.535(5)			<i>a</i> (Å) = 13.522			<i>a</i> (Å) = 13.5 (1)		
<i>b</i> (Å) = 20.606(9)			<i>b</i> (Å) = 20.57(1)			<i>b</i> (Å) = 20.451(1)			<i>b</i> (Å) = 20.608			<i>b</i> (Å) = 20.70(8)		
<i>c</i> (Å) = 4.119(2)			<i>c</i> (Å) = 4.115(2)			<i>c</i> (Å) = 4.104(3)			<i>c</i> (Å) = 4.112			<i>c</i> (Å) = 4.15(1)		
$\alpha = \beta = \gamma = 90^\circ$			$\alpha = \beta = \gamma = 90^\circ$			$\alpha = \beta = \gamma = 90^\circ$			$\alpha = \beta = \gamma = 90^\circ$			$\alpha = \beta = \gamma = 90^\circ$		
Space group: <i>Bbmm</i>			<i>Bbmm</i>			<i>Bbmm</i>			<i>Bbmm</i>			<i>Bbmm</i>		

Data are presented for I: lillianite from Vulcano, Pb/Bi  $\approx$  1.50; II: lillianite from Vulcano, Pb/Bi  $\approx$  1.41; III: a selection of diffraction lines from the calculated powder-diffraction diagram (PDFWIN 71--533), from the crystal structure of natural lillianite (Takeuchi & Tagaki 1972); IV: synthetic Phase III (Otto & Strunz 1968), and V: natural lillianite from Bukuka (Klyachin & Dmitrieva 1968). b: broad lines.

## DISCUSSION

*The lillianite from Vulcano*

Considering the composition of lead-bismuth sulfosalts, Godovikov (1972) noted that natural lillianite

usually incorporates noticeable amounts of different metals. For example, the sample from the Bukuka deposit (eastern Transbaikal, Russia), the homogeneity of which was first supported by X-ray powder-diffraction data (Ontoev 1959, Klyachin & Dmitrieva 1968), contains 2.2 wt% Ag. Makovicky & Karup-Møller (1977b)

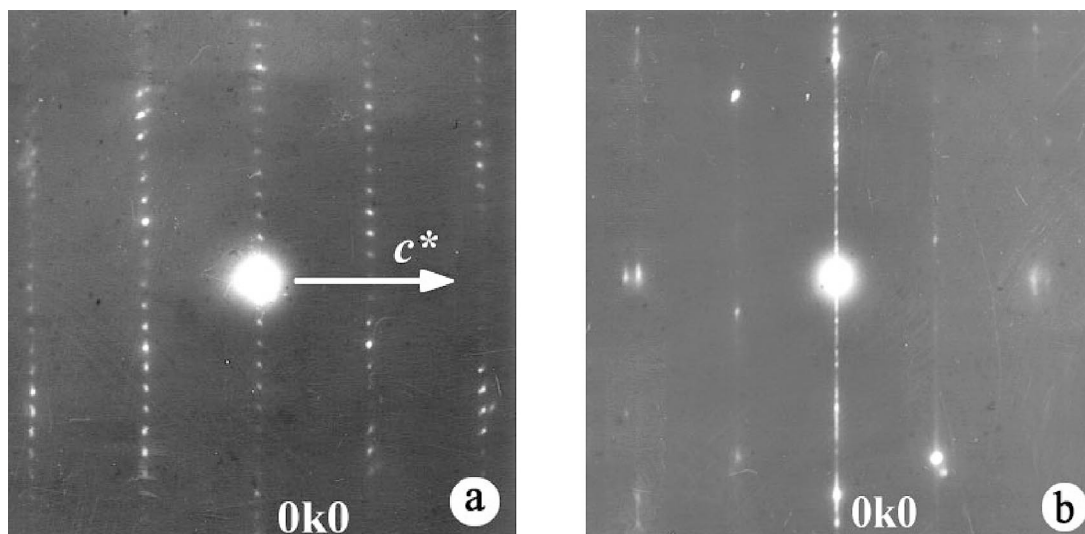


FIG. 4. Electron-microdiffraction photos of lillianite : a) SAED pattern of lillianite with  $b \approx 20.2$  and  $c \approx 4.0$  Å. b) SAED pattern of disordered structure of lillianite with diffuse streaks parallel to  $b^*$ .

and, more recently, Pring *et al.* (1999) reported that no silver-free natural samples of lillianite homologues had been found.

As shown in the chemical data section of the present paper, lillianite from Vulcano has a composition rather close to the ideal one with respect to cations (except for minor incorporation of Cd). Particularly interesting is the absence of Ag and Cu, which allows us to consider the lillianite from Vulcano as unique owing to its relative purity. The lillianite samples show a narrow compositional range caused by slight variations of the main formula-forming cations: Pb and Bi. This has been reflected in the formula:  $\text{Pb}_{3-x}\text{Bi}_{2+2x/3}(\text{S}_{6-y}\text{Se}_y)_{\Sigma 6}$  with  $0 \leq x \leq 0.1$  and  $y \approx 0.25$ , which indicates the extent of departure from the ideal composition  $\text{Pb}_3\text{Bi}_2(\text{S,Se})_6$  toward an increasing Bi content. In terms of the  $\text{Bi}_2\text{S}_3$  mol %, the composition field of samples collected in June 1994 ranges from 24.94 up to 26.65% (with a 1.71% interval). The results of the sixty-six analyses discussed in this paper, as well as the results of a number of analyses of lillianite samples collected from the same fumarole but at different dates (Garavelli & Vurro, unpubl. data), fall within the same range (Fig. 5). These data confirm the existence of nonstoichiometry in lillianite.

The values of chemical N, calculated for the sixty-six analyses presented in this work, range from 3.76 to 4.00 and are mostly not integral and less than the crystallographically defined theoretical value ( $N = 4.00$ ). Makovicky (1981) noted that differences between non-integral values for N, generally smaller than the theoretical one, may be due either to the vacancies ( $\square$ ) in the metal positions, created by substitution  $3\text{Pb}^{2+} \rightarrow$

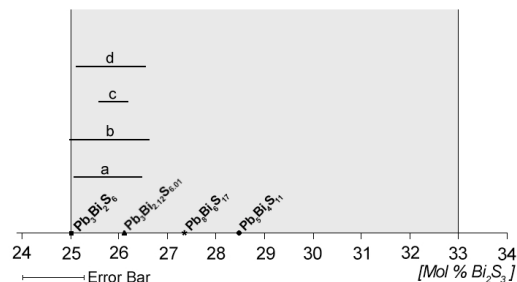


FIG. 5. Comparison of compositions of lillianite from the fumarole FA and synthetic Phase III (in mol.%  $\text{Bi}_2\text{S}_3$ ). In grey: composition field (25–33 mol.%  $\text{Bi}_2\text{S}_3$ ) of Phase III (Salanci & Moh 1969). a) Fumarole FA, June 1994,  $T = 520^\circ\text{C}$ , ARL-SEM-Q95 microprobe. b) Fumarole FA, June 1994,  $T = 520^\circ\text{C}$ , Camebax SX-50 microprobe. c) Fumarole FA, July 1994,  $T = 547^\circ\text{C}$ , ARL-SEM-Q95 microprobe. d) Fumarole FA, October 1992,  $T = 665^\circ\text{C}$ , ARL-SEM-Q95 microprobe. Compositions of Phase III,  $\text{Pb}_3\text{Bi}_2\text{S}_6$ ,  $\text{Pb}_3\text{Bi}_{1.2}\text{S}_{6.01}$  and  $\text{Pb}_5\text{Bi}_4\text{S}_{11}$ , and of bursaitite,  $\text{Pb}_5\text{Bi}_4\text{S}_{11}$ , also are given.

$2\text{Bi}^{3+} + \square$ , or to errors in the frequency of “chemical twinning”. Defect structures and disordered intergrowths were first reported in high-resolution transmission electron microscopy studies on synthetic members of the lillianite homologous series (Skowron & Tilley 1986, Tilley & Wright 1982). Stacking disorder and disordered intergrowth have been recently confirmed also

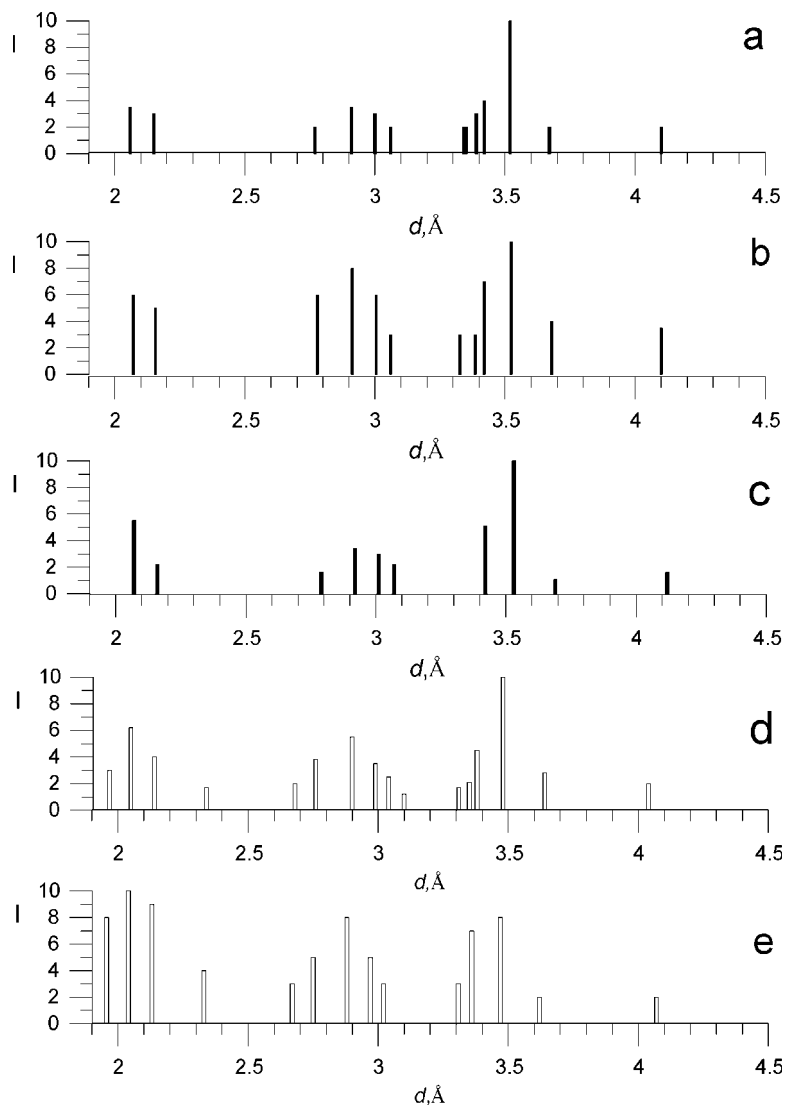


FIG. 6. Schematic diagram of the two types of X-ray powder-diffraction data for synthetic Phase III (main reflections for  $d$  values greater than 2 Å). Type I: a) composition 27 mol.%  $\text{Bi}_2\text{S}_3$  (Pb/Bi = 1.35),  $T = 750^\circ\text{C}$ , evacuated silica-tube experiments (Craig 1967); b) 27.3 mol.%  $\text{Bi}_2\text{S}_3$  (Pb/Bi = 1.33),  $T$  in the range  $750\text{--}800^\circ\text{C}$ , chemical transport method of reaction (Otto & Strunz 1968); c)  $\text{Pb}_3\text{Bi}_{2.12}\text{S}_{6.01}$  (Pb/Bi = 1.42),  $400^\circ\text{C}$ , hydrothermal synthesis (Klyakhin & Dmitrieva 1967). Type II: d) 27.27 mol.%  $\text{Bi}_2\text{S}_3$  (Pb/Bi = 1.33),  $T = 700^\circ\text{C}$ , evacuated silica-tube experiments (Salanci & Moh 1969); e) unknown exact composition,  $T = 750^\circ\text{C}$ , evacuated silica-tube experiments (Godovikov 1972).

in natural equivalents (Pring *et al.* 1999). Taking into account the conditions of formation of the lillianite at Vulcano (high rate of crystallization at the interface between fumarolic fluids and atmosphere), it is reasonable to suppose that the nonstoichiometry of lillianite

studied is mainly due to the same disorder and only to a smaller extent to the vacancy-producing mechanism  $3\text{Pb} \rightarrow 2\text{Bi} + \square$ .

Our X-ray study revealed some differences between the two lillianite crystals, which have different compo-

sitions. A comparison of the set of unit-cell parameters obtained and X-ray powder-diffraction data shows that the differences in parameters  $a$  and  $c$  are in the range of instrumental errors. The value of parameter  $c$  obtained for both the crystals ( $\approx 4.11 \text{ \AA}$ ) agrees with the data reported by Makovicky & Karup-Møller (1977b), who noted that in natural Ag-bearing lillianite, this parameter seems independent of the composition and equal to  $4.11 \text{ \AA}$ . From our analyses, the value of the parameter  $b$  for the crystal with a close-to-ideal composition (Table 4, column I) is the same as that reported by Otto & Strunz (1968) for Phase III, synthetic lillianite (Table 4, column IV). On the other hand, a small but significant decrease in the parameter  $b$  with an increase of Bi content has been recorded. This decrease suggests a variation of this parameter with composition, even though we cannot support this hypothesis on the basis of only two analyses. A similar variation of parameter  $b$  with composition was previously reported by Makovicky & Karup-Møller (1977b), who noted that in natural and synthetic samples of Ag-bearing lillianite, the  $b$  parameter seems linearly dependent on the percentage of the Ag-for-Bi substitution.

Essential differences have been revealed in values of microhardness of the lillianite grains considered (Table 2, No. 1–2 and 7–8). The lower value of microhardness of the Bi-rich sample may be due to the lower degree of order in the structure of the lillianite with the lower value of Pb/Bi, which is consistent with the diffraction data given above. To some extent, the observed decrease may be explained also by the heterovalent substitution  $3\text{Pb}^{2+} \rightarrow 2\text{Bi}^{3+} + \square$ . The structure of lillianite has two independent octahedrally coordinated metal sites,  $M1$  and  $M2$  in the galena-like slabs, and a third one,  $M3$ , in the boundary of the slabs. According to Takagi & Takéuchi (1972), the Pb and Bi atoms are distributed randomly over the  $M1$  and  $M2$  sites, but Ohsumi *et al.* (1984) suggested that the  $M2$  site contains more bismuth than  $M1$ . The  $M3$  site is occupied only by a Pb atom, possibly associated with vacancies. The total number of metal sites per unit cell is 20, with  $Z = 4$ . Taking into account these data, in the case of the Bi-rich sample (Table 2, No. 7–8), we infer about 0.12 vacancies per unit cell, which could contribute to the observed decrease in hardness.

Finally, note that lillianite occurs at Vulcano owing to peculiarities of the deposition environment in fumaroles. The mode of formation of this phase as a sublimate shows some similarities with the conditions of the formation of synthetic Phase III in some hydrothermal experiments. According to Klyakhin & Dmitrieva (1968), synthetic  $\text{Pb}_3\text{Bi}_2\text{S}_6$  is easily crystallized from solutions containing NaCl, KCl and  $\text{NH}_4\text{Cl}$  at 350–450°C. The same compounds play an important role in the fumarole environments at Vulcano, both in the volcanic transport of lead and bismuth as volatile chlorides, and in the early deposition of the same elements as metastable chlorosulfides, from which lillianite and

other sulfosalts form through reactions involving gaseous  $\text{H}_2\text{S}$  (Garavelli *et al.* 1997, Cheynet *et al.* 2000).

#### *Relationships between natural lillianite and its synthetic homologous phases*

The first synthetic “lillianite” was obtained more than 60 years ago (Schenck *et al.* 1939). Later, as the phase relations along the pseudobinary join  $\text{PbS}-\text{Bi}_2\text{S}_3$  of the system  $\text{Pb}-\text{Bi}-\text{S}$  were investigated intensively (Van Hook 1960, Salanci 1965, Craig 1967, Otto & Strunz 1968, Salanci & Moh 1969, Klyakhin & Dmitrieva 1968, Godovikov 1972), Phase III appeared to be the synthetic homologue of lillianite. This phase shows an extensive range of composition, with a maximal solid-solution at 700–750°C. According to Salanci & Moh (1969), its composition ranges from about 25 to 33 mol.%  $\text{Bi}_2\text{S}_3$  at 750°C (Pb/Bi atomic ratio from 1.50 up to 1.02, respectively). The field (Fig. 5) starts approximately from the composition of ideal lillianite,  $\text{Pb}_3\text{Bi}_2\text{S}_6$  (Pb/Bi = 1.50), and covers compositions like  $\text{Pb}_8\text{Bi}_6\text{S}_{17}$  (Pb/Bi = 1.33), initially attributed to gieszenite (Graeser 1963, Strunz 1977),  $\text{Pb}_5\text{Bi}_4\text{S}_{11}$  (Pb/Bi = 1.25), ascribed to bursaite (Ciofflica & Vlad 1974, Strunz 1977, Mozgova *et al.* 1988, Mandarino 1999) and extends approximately to  $\text{Pb}_2\text{Bi}_2\text{S}_5$  (Pb/Bi = 1.00), corresponding to cosalite (Mandarino 1999). The composition of lillianite from Vulcano (Pb/Bi atomic ratio ranging from 1.38 to 1.50, average 1.43) is very similar to the composition of synthetic Phase III of Klyakhin & Dmitrieva (1968)  $\text{Pb}_3\text{Bi}_{2.12}\text{S}_{6.01}$  (Pb/Bi = 1.42 in atoms). This phase, obtained hydrothermally at 400°C, is the synthetic compound better represented by the ideal formula  $\text{Pb}_3\text{Bi}_2\text{S}_6$ .

It is well known that some Pb–Bi sulfosalts are very similar in morphology and physical properties. In addition, the mutual substitution involving occupants of the metal–semimetal positions raise many problems for their definitive identification (Mozgova 1985). For these reasons, the X-ray-diffraction data are considered to provide the most reliable approach. A number of X-ray powder-diffraction data of Phase III, labeled as “synthetic lillianite”, have been published by various authors. Close inspection of published X-ray data for Phase III permits us to distinguish two types, differing in interplanar distances (especially in the region above 2 Å). This is schematically illustrated in Figure 6, where the strongest reflections of the five X-ray powder-diffraction data of Phase III, obtained by different authors using different methods, are represented. The first type (Figs. 6a–c) has two main lines in the low-angle region: 3.52–3.53 and 3.42 Å, whereas the strongest reflections of the second type (Figs. 6d–e) in the same area are 3.47–3.48 and 3.38–3.36 Å. The first type includes the data for Phase III obtained by hydrothermal synthesis (Klyakhin & Dmitrieva 1968), as well as those published by Craig (1967) and Otto & Strunz (1968). As stated above, this type is consistent with the X-ray data

of lillianite from Vulcano. The second type contains the data obtained by Salanci & Moh (1969) and Godovikov (1972). Both of these patterns are very close to that of bursaitite,  $Pb_5Bi_4S_{11}$  (Ciofflica & Vlad 1974, Mozgova *et al.* 1988), which has the strongest reflections at  $d$  values of 3.48 Å ( $I = 10$ ) and 3.38 Å ( $I = 9$ ). On the basis of the data considered, it seems reasonable to suppose that the composition field ascribed to Phase III at 700–750°C is really heterogeneous and probably contains some subphases, as it overlaps the compositional field of Phase V (Takéuchi 1997). These various subphases could be related to the different natural occurrences of lillianite. Some of them have X-ray data that are more similar to the first group of synthetic phases (Craig 1967, Klyakhin & Dmitrieva 1968, Otto & Strunz 1968), whereas the others are closer to the second group of synthetic materials (Salanci & Moh 1969, Godovikov 1972).

#### CONCLUSIONS

This investigation of lillianite samples, recently deposited at the La Fossa crater fumaroles, permits us to report the first natural occurrence of an Ag-free  $^4L$  member of the lillianite homologous series. Its narrow composition field (Pb/Bi atomic ratio ranging from 1.38 to 1.50) is well expressed by the general empirical formula,  $Pb_{3-x}Bi_{2+2x/3}(S_{6-y}Se_y)_{\Sigma 6}$ , with  $0 \leq x \leq 0.1$  and  $y \approx 0.25$ . The observed nonstoichiometry has been mainly attributed to structural disorder and, subordinately, to the simple heterovalent substitution  $3Pb^{2+} \rightarrow 2Bi^{3+} + \square$ . This reconstruction is to be expected in view of the conditions of mineral formation in the exhalative environment.

The chemical composition of lillianite described and X-ray data agree with the data gathered for synthetic Phase III ( $Pb_3Bi_{2.12}S_{6.01}$ , Pb/Bi = 1.42 in atoms) hydrothermally synthesized by Klyakhin & Dmitrieva (1968). Thus at 400–500°C, the compositions of natural Ag-free lillianite and synthetic homologues are close to the accepted ideal formula  $Pb_3Bi_2S_6$ . The other homologous synthetic phases, most of which were obtained by quenching at 700–750°C, contain about 27.3 mol.%  $Bi_2S_3$ , and are better expressed by the formula  $Pb_8Bi_6S_{17}$  (Pb/Bi = 1.33 in atoms). The same formula,  $Pb_8Bi_6S_{17}$ , has been recently used by Liu & Chang (1994) in describing the composition of their synthetic lillianite.

We cannot exclude the possibility that the compositional field of synthetic Phase III, wider at higher temperatures, contains different subphases, as for example Phase V of the same system (Takéuchi *et al.* 1974, 1979, Sugaki *et al.* 1974, Tilley & Wright 1982). Further investigations are required in this regard.

Finally, the occurrence of homogeneous crystals of lillianite at Vulcano lacks traces of decomposition, which are common at other localities (Ontoev 1959, Klyakhin & Dmitrieva 1968). This may be ascribed to the rapid drop in the temperature taking place at the

fumaroles, similar to the quenching procedure in the synthesis of phases in laboratory experiments.

#### ACKNOWLEDGEMENTS

The authors are grateful to two anonymous referees, Associate Editor N.J. Cook and R.F. Martin for their efforts to improve the quality of this paper. Thanks also go to N.I. Organova for her valuable advice and useful discussion of X-ray and electron-diffraction data, to D.K. Shcherbachev for the measurements of the reflectance and microhardness, to N. Mongelli for technical assistance, and to V. Sportelli for revising the English version of our paper. SEM investigations were carried out at Dipartimento Geomineralogico (University of Bari, Italy) using equipment from CNR, Centro Chimica dei Plasmi. This research was performed with the financial support of MURST (Ministero Università e Ricerca Scientifica e Tecnologica, Italy) and National Group for Volcanology, Italy.

#### REFERENCES

- BORODAEV, YU.S., GARAVELLI, A., GARBARINO, C., GRILLO, S.M., MOZGOVA, N.N., ORGANOVA, N.I., TRUBKIN, N.V. & VURRO, F. (2000): Rare sulfosalts from Vulcano, Aeolian Islands, Italy. III. Wittite and cannizzarite. *Can. Mineral.* **38**, 23-34.
- \_\_\_\_\_, \_\_\_\_\_, KUZMINA, O.V., MOZGOVA, N.N., ORGANOVA, N.I., TRUBKIN, N.V. & VURRO, F. (1998): Rare sulfosalts from Vulcano, Aeolian Islands, Italy. I. Se-bearing kirkiite,  $Pb_{10}(Bi,As)_6(S,Se)_{19}$ . *Can. Mineral.* **36**, 1105-1114.
- CHEYNET, B., DALL'AGLIO, M., GARAVELLI, A., GRASSO M.F. & VURRO, F. (2000): Trace elements from fumaroles at Vulcano Island (Italy): rates of transport and a thermochemical model. *J. Volcanol. Geotherm. Res.* **95**, 273-283.
- CHUKHROV, F.V. (1960): *Minerals. 1. Handbook*. Publishing House Academy of Sciences of USSR, Moscow, Russia (in Russ.).
- CIOFFLICA, G. & VLAD, S. (1974): The occurrence of bursaitite in skarn deposits from Băița Bihorului (Apuseni Mountains). *Revue Roum. Géol. Géophys. et Géogr., Géologie* **18**, 3-7.
- CRAIG, J.R. (1967): Phase relations and mineral assemblages in the Ag–Bi–Pb–S system. *Mineral. Deposita* **1**, 278-306.
- CRIDDLE, A.J. & STANLEY, C.J. (1993): *Quantitative Data File for Ore Minerals* (3rd ed.). Chapman & Hall, London, U.K.
- FLEISCHER, M. (1969): New mineral names. *Am. Mineral.* **54**, 579.
- GARAVELLI, A. (1994): *Mineralogia e Geochimica di fasi vulcaniche condensate. I sublimati dell'Isola di Vulcano tra il 1990 ed il 1993*. Ph.D. thesis, Dipartimento Geomineralogico, Università degli Studi di Bari, Bari, Italy.

- \_\_\_\_\_, LAVIANO, R. & VURRO, F. (1997): Sublimate deposition from hydrothermal fluids at the Fossa crater – Vulcano, Italy. *Eur. J. Mineral.* **9**, 423-432.
- GODOVIKOV, A.A. (1972): Bismuth sulfosalts: their chemical composition, synthesis and classification. In Peculiarities of the Chemical Composition, Synthesis, Classification. Nauka, Moscow, Russia (in Russ.).
- GRAESER, S. (1963): Giessenit – ein neues Pb–Bi Sulfosalz aus dem Dolomit des Binntales. *Schweiz. Mineral. Petrogr. Mitt.* **43**, 471-478.
- KELLER, H.F. (1890): IV. Ueber Kobellit von Ouray, Colorado, und über die chemische Zusammensetzung dieser Species. *Z. Kristallogr.* **17**, 67-72.
- \_\_\_\_\_, & KELLER, H.A. (1885): A new variety of kobellite. *J. Am. Chem. Soc.* **7**, 194-195.
- KLYAKHIN, V.A. & DMITRIEVA, M.T. (1968): More information about synthetic and natural lillianite. *Dokl. Acad. Sci. USSR, Earth Sci. Sect.* **178**, 106-108.
- KUPČIK, V., FRANC, L. & MAKOVICKY, E. (1969): Mineralogical data on a sulphosalt from the Rhodope Mountains, Bulgaria. *Tschermaks Mineral. Petrogr. Mitt.* **13**, 149-156.
- LIU, HUIFANG & CHANG, L.L.Y. (1994): Lead and bismuth chalcogenide systems. *Am. Mineral.* **79**, 1159-1166.
- MAKOVICKY, E. (1977): Chemistry and crystallography of the lillianite homologous series. III. Crystal chemistry of lillianite homologues. Related phases. *Neues Jahrb. Mineral., Abh.* **131**, 187-207.
- \_\_\_\_\_, (1981): The building principles and classification of bismuth–lead sulphosalts and related compounds. *Fortschr. Mineral.* **59**, 137-190.
- \_\_\_\_\_, & KARUP-MØLLER, S. (1977a): Chemistry and crystallography of the lillianite homologous series. I. General properties and definitions. *Neues Jahrb. Mineral., Abh.* **130**, 264-287.
- \_\_\_\_\_, & \_\_\_\_\_ (1977b): Chemistry and crystallography of the lillianite homologous series. II. Definition of new minerals: eskimoite, vikingite, ourayite and treasurerite. Redefinition of schirmerite and new data on the lillianite–gustavite solid-solution series. *Neues Jahrb. Mineral., Abh.* **131**, 56-82.
- MANDARINO, J.A. (1999): *Fleischer's Glossary of Mineral Species 1999*. The Mineralogical Record, Inc., Tucson, Arizona
- MOZGOVA, N.N. (1985): *Non-Stoichiometry and Homologous Series of Sulphosalts*. Nauka, Moscow, Russia (in Russ.).
- \_\_\_\_\_, KUZMINA, O.V., ORGANOVA, N.I., LAPUTINA, I.P., BORODAEV, YU.S. & FORNASERI, M. (1985): New data on sulfosalts assemblages at Vulcano (Italy). *Rend. Soc. It. Mineral. Petrol.* **40**, 277-283.
- \_\_\_\_\_, ORGANOVA, N.I., BORODAEV, YU.S., RYABEVA, E.G., SIVITSOV, A.V., GETMANSKAYA, T.I. & KUZMINA, O.V. (1988): New data on cannizzarite and bursaite. *Neues Jahrb. Mineral., Abh.* **158**, 293-309.
- OHSUMI, K., TSUTSUI, K., TAKÉUCHI, Y. & TOKONAMI, M. (1984): Reinvestigation of lillianite structure with synchrotron radiation. *Acta Crystallogr.* **40A** (Suppl.), C255-C256.
- ONTOEV, D.O. (1959): Lillianite from Bukuka deposit and conditions under which it formed. *Dokl. Acad. Sci. USSR, Earth Sci. Sect.* **126**, 891-593.
- OTTO, H.H. & STRUNZ, H. (1968): Zur Kristallchemie synthetischer Blei–Wismut–Spießglanze. *Neues Jahrb. Mineral., Abh.* **108**, 1-19.
- PRING, F., JERCHER, M. & MAKOVICKY, E. (1999): Disorder and compositional variation in the lillianite homologous series. *Mineral. Mag.* **63**, 917-926.
- SALANCI, B. (1965): Untersuchungen am System Bi<sub>2</sub>S<sub>3</sub> – PbS. *Neues Jahrb. Mineral., Monatsh.*, 384-388.
- \_\_\_\_\_, & MOH, G.H. (1969): Die experimentelle Untersuchung des pseudobinären Schnittes PbS–Bi<sub>2</sub>S<sub>3</sub> innerhalb des Pb–Bi–S-Systems in Beziehung zu natürlichen Blei–Wismut–Sulfosalzen. *Neues Jahrb. Mineral., Abh.* **112**, 63-95.
- SCHENCK, R., HOFFMANN, I., KNEPPER, W. & VOLGER, H. (1939): Gleichgewichtsstudien erzbildende Sulphide, I. *Z. anorg. allg. Chem.* **240**, 173-197.
- SHCHERBACHEV, D.K. (1998): About two approaches to the microhardness investigation by the Ludvig–Vickers' method. *Zap. Vser. Mineral. Obshchest.* **127**(2), 119-126 (in Russ.).
- SKOWRON, A. & TILLEY, R.J.D. (1986): The transformation of chemically twinned phases in the PbS–Bi<sub>2</sub>S<sub>3</sub> system to the galena structure. *Chemica Scripta* **26**, 353-358.
- STRUNZ, H. (1977): *Mineralogische Tabellen*. Akademische Verlagsgesellschaft Geest & Portig K.-G., Leipzig, Germany.
- SUGAKI, A., SHIMA, H. & KITAKAZE, A. (1974) : Synthetic phases in the PbS–Bi<sub>2</sub>S<sub>3</sub> system; PbBi<sub>4</sub>S<sub>7</sub> and Pb<sub>2</sub>Bi<sub>2</sub>S<sub>5</sub>. *Technol. Rep., Yamaguchi Univ.* **1**, 369-373.
- TAKAGI, J. & TAKÉUCHI, Y. (1972): The crystal structure of lillianite. *Acta Crystallogr.* **B28**, 649-651.
- TAKÉUCHI, Y. (1997): *Tropochemical Cell-Twinning: a Structure-Building Mechanism in Crystalline Solids*. Terra Scientific Publ. Co., Tokyo, Japan.
- \_\_\_\_\_, OZAWA, T. & TAKAGI, J. (1979): Tropochemical cell-twinning and the 60 Å structure of phase V in the PbS–Bi<sub>2</sub>S<sub>3</sub> system. *Z. Kristallogr.* **150**, 75-84.

- \_\_\_\_\_, TAKAGI, J. & YAMANAKA, T. (1974) : Structural characterization of the high-temperature phase V on the PbS–Bi<sub>2</sub>S<sub>3</sub> join. *Z. Kristallogr.* **140**, 249-272.
- TILLEY, R.J.D. & WRIGHT, A.C. (1982): Chemical twinning in the PbS region of the PbS–Bi<sub>2</sub>S<sub>3</sub> system. *Chemica Scripta* **19**, 18-22.
- VAN HOOK, H.J. (1960): The ternary system Ag<sub>2</sub>S–Bi<sub>2</sub>S<sub>3</sub>–PbS. *Econ. Geol.* **55**, 759-788.
- VURRO, F., GARAVELLI, A., GARBARINO, C., MOÉLO, Y. & BORODAEV, YU.S. (1999): Rare sulfosalts from Vulcano, Aeolian Islands, Italy. II. Mozgovaite, PbBi<sub>4</sub>(S,Se)<sub>7</sub>, a new mineral species. *Can. Mineral.* **37**, 1499-1506.
- WAGNER, R.S. & ELLIS, W.C. (1965): The vapor–liquid–solid mechanism of crystal growth and its application to silicon. *Trans. Metall. Soc. AIME* **233**, 1053-1064.

*Received October 28, 2000, revised manuscript accepted July 22, 2001.*